Journal of Marine Systems
June 2020, Volume 206, Pages 103307 (9p.)
https://doi.org/10.1016/j.jmarsys.2020.103307
https://archimer.ifremer.fr/doc/00600/71238/

Early-life ontogenetic developments drive tuna ecology and evolution

Aoki Yoshinori [1, *], Jusup Marko [2], Nieblas Anne-Elise [3], Bonhommeau Sylvain [3], Kiyofuji Hidetada [1], Kitagawa Takashi [4]

[1] National Research Institute of Far Sea Fisheries, Japan Fisheries Research and Education Agency, Shimizu, Shizuoka, Japan
[2] Institute of Innovative Research, Tokyo Institute of Technology, Tokyo 152-8552, Japan
[3] IFREMER (Institut Français de Recherche pour l'Exploitation de la MER), 34203 Sète Cedex, France
[4] Atmosphere and Ocean Research Institute, The University of Tokyo, Kashiwanoha, Kashiwa, Chiba 277-8564, Japan

* Corresponding author : Yoshinori Aoki, email address : aokiyoshinori@affrc.go.jp

Abstract :

Formal approaches to physiological energetics, such as the Dynamic Energy Budget (DEB) theory, enable interspecies comparisons by uniformly describing how individuals of different species acquire and utilise energy. We used the DEB theory to infer the energy budgets of three commercial tuna species (skipjack, Pacific bluefin, and Atlantic bluefin) throughout all stages of ontogenetic development—from an egg to an adult individual and its eggs. Energy budgets were inferred from exhaustive datasets fed into a DEB-based mathematical model tailored for tuna fish until reaching a high goodness of fit and thus reliable estimates of the model parameters. The life histories of all three species are strongly influenced by morphological and physiological adaptations that accelerate ontogeny during the larval stage, although the effect is more pronounced in bluefin than skipjack tuna. Accelerated ontogeny in energetic terms is a simultaneous improvement of energy acquisition (higher intake) and utilisation (higher expenditure) without changing the capacity of fish to build energy reserve as intake and expenditure increase in unison. High energy expenditure, an even higher intake by necessity, and a limited capacity to build energy reserve, make all three tuna species vulnerable to starvation, thereby theoretically underpinning the description of tuna as “energy speculators”. Energy allocation to reproduction maximises fecundity of all three tuna species, thus suggesting that the evolution of tuna favours higher fecundity at the expense of growth. Thinking beyond just physiological energetics (e.g., wild stock projections), DEB-based models are a natural foundation for physiologically-structured population dynamics wherein the environment influences the population growth rate via metabolism.

Highlights

► We inferred energy budgets of skipjack, Pacific bluefin, and Atlantic bluefin tuna. ► Morphological and physiological adaptations accelerate ontogeny in the larval stage. ► Accelerated ontogeny expands tuna scope for growth, but leaves energy reserve small. ► Thermogenesis that starts in early juveniles is a considerable energy sink. ► Large body, small reserve, and high energy costs shape tuna ecology and evolution.

Keywords : accelerated ontogeny, bluefin tuna, Dynamic Energy Budget theory, ecology and evolution, energy speculators, skipjack tuna

1. Introduction

Understanding life-history traits of marine animals in terms of physiological constraints is fundamentally important for inferring their ecological function and role among species. Commercial tuna species have received particular attention in this context because of their unique life-history traits among teleosts and a captivating functional evolution, including large size, elevated body temperature, and exceptional swimming ability (e.g., Carey & Teal, 1966; Graham & Dickson, 2004). Despite sharing some general traits, tuna species differ between themselves in terms of body length, body mass, life span, and fecundity (e.g., Matsumoto et al., 1984; Santamaria et al., 2009). In peer-reviewed literature, for example, the maximum reported body length of skipjack tuna (SKJ; *Katsuwonus pelamis*) is only 94 cm (Matsumoto et al., 1984), while that of Pacific bluefin tuna (PBT; *Thunnus orientalis*) and Atlantic bluefin tuna (ABT; *Thunnus thynnus*) is 265 cm (Masuma, 2009) and 372 cm (Santamaria et al., 2009), respectively. A rich body of respirometry-based literature has laid the groundwork for the basic understanding of tuna life-history traits (e.g., Dewar & Graham, 1994; Korsmeyer et al., 1996), but relatively few studies have taken a comprehensive, full life cycle perspective (*sensu* Jusup et al., 2011; Jusup et al., 2014) to explain the differences between species in terms of physiological constraints. Herein we seek to fill this latter gap in particular.

Comparative physiology has relied on a multitude of methodologies to study the diversity of functional characteristics of organisms (Garland & Carter, 1994). While there is no single preferred methodology, we used the principles of physiological energetics (Jusup & Matsuda, 2015) as a basis for comparing three commercial tuna species: Atlantic bluefin, Pacific bluefin, and skipjack. More specifically, we based our study on the general framework of Dynamic Energy Budget (DEB) theory for building individual-based energetics models

(Nisbet et al., 2000; Kooijman, 2010; Jusup et al., 2017). DEB theory derives metabolic processes of an organism as a function of food intake and temperature from the first principles (e.g., mass-energy conservation laws, homeostasis of organisms, etc.). The theory, furthermore, specifies interspecies scaling relationships (Kooijman, 2010; Jusup et al., 2017) needed to explain the well-known patterns in the measured field data (e.g., Schmidt-Nielsen, 1972). Here, we seek to identify the mechanistic origins of the large differences in, e.g., body size between tunas, but also to understand the mechanisms from which common tuna life-history traits arise.

We built on an existing (Jusup et al., 2011), calibrated and validated (Jusup et al., 2014), full life cycle model for PBT—from an egg to an adult individual and its eggs. We updated the parameters of this model to capture additional minute details of the PBT life-history (e.g., egg dry mass), and then used the resulting parameter values in conjunction with the covariation method (Lika et al., 2011) to adapt the same model to SKJ and ABT. We then reconstructed the energy budgets of all three species and described the probable mechanisms behind various tuna life-history traits. Finally, we discussed these results in terms of tuna physiology, ecology, and evolution.

2. Materials and methods

2.1 Model outline

Because a comprehensive description of the DEB model for tuna can be found elsewhere in the literature (Jusup et al., 2011, 2014), here we focus on the key concepts and give further mathematical details in the Supporting Information (SI) Methods. Conceptually, all DEB models can be characterised by the equation

$$\frac{dL}{da} = G(i-state, e-state), \quad \textbf{(1)}$$

where L is fish size, a is age, and $\dot{G}=\dot{G}$(*i-state*, *e-state*) is a growth function that depends on the state of this fish (*i-state*), as well as the environmental conditions (*e-state*), primarily food and temperature. In DEB theory, the set of *i-state* variables includes reserve energy E, maturity E_H, and size L.

Reserve tissues (quantified by E) serve as an intermediate storage for ingested energy from which all metabolic processes are powered except the ingestion itself. Because of their transient role, these tissues are not maintained. By contrast, structural tissues (quantified by L) are indispensable for survival and hence continuously maintained. Both variables L and E are *material* because the tissues that they quantify contribute to the body mass of the fish. Maturity E_H is structure-like in that it requires maintenance, but is *immaterial* in the sense that energy invested into maturation in embryo, larval, and juvenile stages is dissipated as heat and metabolites into the environment in order to prepare the organism for the adult stage. Intuitively, E_H can be seen as a sort of biological clock (Augustine, 2017), whereby the fish switches between life stages when the certain threshold values of maturity are reached. In the adult stage, energy previously invested into maturation is redirected to reproduction.

Each of the three *i-state* variables—E, L, and E_H—has a corresponding first order differential

equation in age, a (SI Methods). This means that on the left-hand side of each equation is the age derivative of one state variable, while on the right-hand side are energy flows between the fish and the environment (assimilation and dissipation) and between tissues (growth). All energy flows are generally functions of *i-state* and *e-state* variables, as well as a number of model parameters, each of which has a specific mechanistic interpretation.

The standard DEB theory recognizes six energy flows (Fig. S1). Assimilation flow, $\dot{p}_A$, is a continuation of food intake after accounting for the digestive system's inefficiencies and overhead costs due to the conversion of food into reserve tissues. Utilization flow, $\dot{p}_C$, determines the rate at which energy is drawn from the reserve to power the remaining metabolic processes. Fraction $\kappa\dot{p}_C$, $0<\kappa<1$, of the utilization flow is allocated to somatic energy needs, while the remaining fraction, $(1-\kappa)\dot{p}_C$, is allocated to maturation or, in the adult stage, reproduction. Somatic energy needs consist of the maintenance of structure, $\dot{p}_S$, and growth, $\dot{p}_G$, if $\dot{p}_G=\kappa\dot{p}_C-\dot{p}_S>0$. If this condition of positive growth cannot be satisfied, the fish is experiencing a food shortage (i.e., starvation) during which we assume $\dot{p}_G=0$. In analogy with somatic energy needs, fraction $(1-\kappa)\dot{p}_C$ of the utilisation flow is used for maturity maintenance, $\dot{p}_J$, and maturation, $\dot{p}_R$, if $\dot{p}_R=(1-\kappa)\dot{p}_C-\dot{p}_J>0$. In the adult stage, $\dot{p}_R$ is the rate of gonad production if the fish continuously reproduces (SKJ), or the rate of energy accumulation in a reproductive buffer in preparation for the next reproductive season (PBT and ABT). In the latter case, the state of the reproductive buffer must be tracked using an auxiliary state variable, E_R, which is also material because it reflects the amount of reserve tissue provisioned for the purpose of gonad production.

2.2 Converting model state variables to measured data

We linked the state variables of the tuna DEB model to measured data (SI Methods) via several conversions. Fork length L_W, for example, was related to structural length L via the

shape factor, δ_M. This factor can be considered constant if growth is approximately isometric. Studied tunas do grow nearly isometrically after the early juvenile stage, but larvae and early juveniles change their shape in a substantial way (Miyashita et al., 2001), which had to be taken into account. Accordingly, we incorporated the changing body shape into the model by transforming the shape factor into a function of maturity, $\delta_M = \delta_M(E_H)$, thus yielding

$$L_W = \frac{L}{\delta_M(E_H)}. \quad (2)$$

The shape factor's functional form (SI Methods) was such that its value increased relatively fast during the early ontogeny, but became progressively more saturated afterwards.

We calculated wet body mass by summing up contributions from material state variables: structure (L), reserve (E), and—for bluefin tunas—the reproductive buffer (E_R) (Jusup et al., 2011). For skipjack tuna, we assumed nearly continuous reproduction, meaning that the reproductive buffer's contribution to body mass was negligible ($E_R \approx 0$). Consequently,

$$W = d_v L^3 + \rho_E (E + E_R), \quad (3)$$

where d_v is structural density assumed ≈1.0 g·cm^{-3}, and ρ_E is a reserve mass-energy coupler estimated at $1.0864 \cdot 10^{-4}$ g·J^{-1} (Jusup et al., 2014).

We obtained batch fecundity, $\dot{F}$, by dividing energy allocated to the reproductive buffer (E_R) with the total number of batches per year, N, and the initial energy reserve of an egg, E_0. Accordingly,

$$F = \frac{\kappa_R \times E_R}{N \times E_0}, \quad (4)$$

where κ_R is efficiency with which the mother's reserve gets converted into eggs. This efficiency is typically set to a high value ($\kappa_R \approx 0.95$) because the mother's reserve and reserve energy stored into an egg should have similar chemical compositions. Calculating initial

energy reserve E_0 is a technically demanding task, and the detailed procedure can be found in the literature (Kooijman, 2009; Jusup et al., 2017).

2.3 Physiologically and ecologically relevant quantities

Based on the DEB model parameters, we calculated the ultimate size using

$$L_\infty = \frac{\kappa M_1\{\dot{p}_{Am}\}}{[\dot{p}_M]} f - \frac{\{\dot{p}_T\}}{[\dot{p}_M]}, \qquad (5)$$

which mechanistically underpins various energetic contributions to body size. For example, κ is allocation to somatic maintenance and growth as opposed to maturation (maintenance) and reproduction. The more the fish allocate to growth, the larger they get. Similarly, $M_1\{\dot{p}_{Am}\}$ is the overall surface-area-specific assimilation rate, where the value of M_1 reflects the effects of morphological and physiological changes in the larval stage on energy assimilation and utilisation. Higher assimilation also makes fish larger. Quantity f reflects food availability in the environment, where f=1 (f=0) signifies unlimited (no) food. More abundant food, of course, fuels more growth. Finally, $[\dot{p}_M]$ and $\{\dot{p}_T\}$ are volume-specific somatic maintenance rates. Maintenance dissipates energy in terms of heat and metabolites, thus leaving less for growth.

Another quantity of interest is reserve turnover time, $t=[E_m]/[\dot{p}_C]$. Here, $[E_M]=\{\dot{p}_{Am}\}/\dot{v}$ represents reserve capacity, where the energy conductance, $\dot{v}$, is a model parameter characterising the rate of energy utilisation from reserve. By definition, $[\dot{p}_C]=\dot{p}_C/L^3$. A quantity related to turnover time is the time to reserve depletion, which indicates the degree of vulnerability to food-poor environments. We assumed that starvation was triggered when food availability barely satisfied somatic maintenance costs, i.e., when $\kappa\dot{p}_C=\dot{p}_S$, at which point energy left in reserve was $E^*=\dot{p}_S L/\kappa\dot{v}$. We further assumed that this energy was used solely to pay the somatic maintenance cost, in which case the time to reserve depletion was given by

$t = E^*/\dot{p}_S = L/\kappa\dot{v}$. Large individuals better handle starvation. Alternatively, $t = L/\kappa\dot{v} \times (\dot{p}_S/(\dot{p}_S + \dot{p}_J))$ if energy is used to pay both somatic and maturity maintenance costs.

To assess the reproductive potential of the three studied species, we calculated fecundity of an individual at maximum structural length, L_m, relative to theoretical maximum fecundity at this length as a function of allocation to soma, κ. We obtained an expression for L_m by inserting f=1 into Eq. (5). We subsequently substituted an expression for the cumulative energy invested in reproduction at L_m,

$$E_R = \int \left(\frac{1-\kappa}{\kappa}([\dot{p}_M]L_m + \{\dot{p}_T\})L_m^2 - \dot{k}_j E_H^p\right)dt, \quad \textbf{(6)}$$

into Eq. (4) to obtain fecundity at L_m as a function of κ. This function attains a maximum value for particular $\kappa=\kappa_0$, which we used to normalise the results and express them in percentages.

3. Results

3.1 Goodness of fit

The tuna DEB model produces satisfactory fits to exhaustive datasets (Table S1) that encompass the whole lifecycle of all three tuna species (Figs. 1, 2; Table 1). Using a goodness-of-fit (GOF) scale from 0 for a complete mismatch to 100 for a perfect fit (SI Methods), we find that GOF_{SKJ}=90.1, GOF_{PBT}=95.0, and GOF_{ABT}=93.0, thus quantitatively confirming that the model's precision is favourable for all three studied species.

In the embryonic stage, hatching as a function of temperature (Fig. 1a), egg dry mass, length at hatching, and length at birth (i.e., first feeding; Table 1) are all estimated by the model with favourable accuracy. The model simulates well the near-exponential growth in the larval stage (Fig. 1b), and the sudden deceleration of growth early in the juvenile stage (Fig. 1c). These growth curves are accompanied with the reasonable estimates of weight-length relationships in the juvenile stage (Fig. 2a).

A number of tuna life-history traits characterising the adult stage are also successfully estimated by the model (Table 1). These traits include length at puberty, ultimate length, and ultimate body mass. Furthermore, growth in the adult stage of all three tuna species is well approximated by the von Bertalanffy growth curve (Fig. 1d). This growth curve is a distinct solution of the underlying model obtained when food availability, f, and temperature, T, are kept constant (Jusup et al., 2017). It is important in this context that our modelling framework uses time-averaged energy flows; these flows change on weekly or monthly time scales (Marques, 2017), thus smoothing out variable environmental conditions experienced by tuna on short time scales of hours or days (Aoki et al., 2017).

In addition to the growth curves, the model is successful at simulating the adult stage weight-length relationships for all three tuna species (Fig. 2b). These relationships differ between

SKJ, and PBT and ABT because the former is a tropical species that reproduces throughout the year (Hunter et al., 1986) and the latter are temperate species that reproduce during a relatively short reproductive season (Kitagawa et al., 2010). A consequence is that SKJ need not, whereas PBT and ABT need to accumulate energy for reproduction, which is in the model idealised as either absence or presence of the reproductive buffer.

Much like the state of the reproductive buffer, the reproductive output in terms of batch fecundity is controlled by the investment of energy into reproduction. Batch fecundity as a function of body length is accurately estimated by the model (Fig. 2c), and together with the estimated number of batches per year (Table S3), indicates that the tropical SKJ spawn on average 30 batches annually, while the temperate PBT and ABT spawn eight to nine batches per reproductive season. The annual reproductive output of SKJ thus reaches up to 40 millions eggs. PBT and ABT may respectively spawn in excess of 240 and 360 million eggs in a single reproductive season.

3.2 Energy budgets

Relating various energy expenditures to energy assimilation, and displaying this as a function of body size, provides an insight into the energy budgets of the three studied species (Fig. 3). These budgets exhibit similar qualitative characteristics, but quantitative differences arise as a consequence of the different parameter values.

Energy budgets in Fig. 3 are dominated by allocation to soma (i.e., the sum of somatic maintenance and growth flows). We find a strong preference for growth early on in the life cycle, but when a certain body size is reached, somatic maintenance takes over. Such an allocation strategy enables rapid growth during the most vulnerable (i.e., larval and early juvenile) stages of life, as well as an extreme migratory lifestyle conducive of high predation by tunas in later stages. The reason for this latter claim is that somatic maintenance in our

model includes the energetic expenditure of excess red muscle unique to tuna physiology which is believed to be the motor behind long-distance tuna migrations (Watanabe et al., 2015) and the heat pump powering tuna thermogenesis (Carey & Teal, 1966). Interestingly, the nonlinear increase in the proportion of energy budget attributed to somatic maintenance coincides with the decelerating growth rates in the juvenile stage of all three species (Fig. 1b), but also corresponds closely to the timing of excess red muscle development in the ontogeny of juvenile tuna (Kubo et al., 2008). By the time the excess red muscle and thermogenesis are fully operational (19.7 cm, 36.8 cm, and 44.1 cm fork length for SKJ, PBT, and ABT, respectively), somatic maintenance accounts for 67.3%, 63.2%, and 63.7% of the total assimilated energy in SKJ, PBT, and ABT, respectively. Thereafter somatic maintenance scales linearly with size, giving rise to the familiar von Bertalanffy growth curve throughout most of the tuna life cycle.

Turning attention to the reproductive branch of tuna energy budgets (i.e., the sum of maturation/reproduction and maturity maintenance flows), we find that investments into maturation and, consequently, maturity maintenance accelerate relative to assimilation at the same time as the investment into somatic maintenance (Fig. 3). This result is a consequence of the relationship between somatic maintenance and utilisation energy flows whereby an increase in the former flow also speeds up the latter one. Furthermore, because the utilisation flow powers all metabolic processes apart from assimilation (Fig. S1), more energy becomes available for maturation, which is then closely followed by a larger demand for maturity maintenance.

An interesting feature of all three energy budgets is that maturity maintenance needs gradually outpace the investment into maturation in the juvenile stage. Maturity maintenance peaks towards the onset of the adult stage, at which point there is a slim margin for further

maturation, especially in the case of two bluefin tunas (Fig. 3b,c). This observation suggests that even a relatively small worsening in the environmental conditions of PBT or ABT may considerably prolong their time to maturation or even compromise the ability to mature at all. This is evidenced by a comparison of growth (Fig. 1d) and maturation of captive and wild PBT (SI Results). The former mature two years earlier than the latter primarily due to a higher temperature experienced in captivity. Further analysis in terms of supply stress (SI Results) reveals the true extent to which the energy budgets of bluefin tunas are constrained (Fig. S5). Finally, that feeding can severely affect bluefin tuna maturation is also found in the data from captivity (Jusup et al., 2014). Once the adult stage is reached, however, maturation and thereby maturity maintenance become fixed, which leaves an increasing amount of energy for reproduction as fish grow bigger.

Energy budgets provide a first indication that tunas may possess reserve with an exceptionally low capacity and thus a high associated turnover. This is reflected in the narrow bands of energy remaining to build up reserve as a difference between assimilation and utilisation.

3.3 Reserve capacity, turnover, and time to depletion

Reserve capacity is another ecologically important variable because it determines the resilience of an individual fish in the face of adverse feeding conditions. Given the relatively large size of tunas (SI Results), based on DEB theory and its interspecies body-size scaling relationships (Nisbet et al., 2000; Jusup et al., 2017), one might expect that the largest constituent of body mass is reserve. Surprisingly, reserve contributes only 15%, 9%, and 11% to body mass of SKJ, PBT, and ABT, respectively (Fig. 4a). To put this result into perspective, we compare the maximum reserve energy density of 1806 $J \cdot cm^{-3}$, 1103 $J \cdot cm^{-3}$, and 1371 $J \cdot cm^{-3}$ calculated for SKJ, PBT, and ABT, respectively, to a maximum reserve

density of 12791 $J \cdot cm^{-3}$ estimated for loggerhead turtles. Although the turtle's ultimate size is approximately 96 cm, there exists an order of magnitude difference in maximum reserve density relative to tuna. Accordingly, reserve contributes to over 60% of loggerhead turtle body mass (Marn et al., 2017).

Structure is by far the largest contributor to tuna body mass, reaching about 80% in all three studied species (Fig. 4a). Given that structure requires maintenance and contributes to such a large percentage of body mass, tunas may be unable to handle starvation for prolonged periods of time. Some empirical evidence to this effect already exists in the literature (Boggs and Kitchell, 1991). We calculated reserve turnover time to provide an indication in this context. The results reveal turnover times of 0.9 days for SKJ and PBT, and 0.6 days for ABT at the moment of entering the juvenile stage. These values increase to 8.3 days for SKJ, 15.8 days for PBT, and 14.3 days for ABT at the moment of sexual maturation. Finally, the largest individuals have reserve turnover times of 20.2 days for SKJ, 24.2 days for PBT, and 32.4 days for ABT. It therefore appears that young tunas are particularly vulnerable to starvation. To give a rough estimate of how long these fish may endure without feeding, we also calculated the time to reserve depletion under starvation (f=0; Fig. 4b). When body size reaches about 20% of ultimate length, which amounts to 19 cm fork length for SKJ, 49 cm fork length for PBT, and 67 cm fork length for ABT, the time to reserve depletion is 4.4 days, 5.3 days, and 9.5 days, respectively, indicating that small tunas are extremely sensitive to feeding conditions. The situation somewhat improves for large fish near their ultimate size because they have 22 days, 26 days, and 48 days, respectively, before running out of reserve energy. These calculations excluded any behavioural adaptations to starvation, as well as the possible reliance of large bluefin tunas on energy in the reproductive buffer.

The presence or absence of a reproductive buffer, and of the corresponding contribution to

body mass (Fig. 4a), is a consequence of the different spawning habits of SKJ as opposed to bluefin tunas. Namely, SKJ is capable of spawning throughout the year, in which case we assume that the reproductive buffer contributes only an indiscernible amount to body mass. By contrast, PBT and ABT spawn only during a limited time window, requiring considerable energy accumulation in preparation for the spawning season. This energy contributes to, on average, about 9% of PBT body mass and 13% of ABT body mass.

3.4 Reproductive potential

Energy allocated to reproduction determines fecundity which, alongside survival, plays a key role in population ecology. The shape of the model-estimated fecundity at maximum length as a function of allocation to soma (parameter κ) relative to the theoretical maximum achieved at the optimal κ value is concave (Fig. 5) because for small κ, severely limited growth also limits energy intake, leading to a chronic lack of energy for allocation to reproduction. For large κ, by contrast, almost all energy is invested into soma in spite of the relatively high intake, leaving just a tiny amount for reproduction. The optimal fecundity is thus reached for intermediate κ values. Interestingly, the estimated κ value for all three studied species is very near their respective optima. This result has an important evolutionary implication discussed below.

4. Discussion

We developed novel Dynamic Energy Budget (DEB) models for skipjack (SKJ) and Atlantic bluefin (ABT) tunas, as well as updated a previously published model for Pacific bluefin tuna (PBT; Jusup et al., 2011, 2014). These models successfully fit the data from all life stages of the three studied species—from an egg to an adult individual and its eggs—revealing in the process the underlying physiological energetics in terms of environment-dependent energy budgets. Here, we primarily focus on comparing the energy budgets corresponding to the present environmental conditions experienced by tunas in the wild. Promising future research directions are located in the SI Discussion.

4.1 Implications of accelerated ontogeny in tuna larvae

Morphological and physiological transformations in the larval stage strongly influence life histories of all three studied species. The morphological transformations in question include allometric (as opposed to isometric) growth of preanal length, head length, head height, snout length, upper jaw length, and eye diameter (Miyashita et al., 2001). Collectively, these transformations point to considerable improvements in energy ingestion. This is further accompanied with simultaneous physiological transformations, such as the first appearance and increase in the number of gastric glands and pyloric caeca, as well as marked jumps in the activity of trypsine-like and pepsine-like digestive enzymes (Kaji, 2003), which suggest improvements in energy assimilation. The physiological transformations that point to improvements in energy utilisation include an increasing ratio of growth hormone immunoreactive cells volume to pituitary volume as an indicator of growth hormone activity and an increasing RNA-to-DNA ratio as an indicator of protein synthesis (Kaji, 2003).

The described transformations, simply put, accelerate tuna ontogeny by simultaneously increasing energy assimilation and utilisation rates. Consequently, larval tuna experience a pe-

riod of near-exponential growth, followed by a period of fast growth of early juveniles at a near constant rate until approximately four months old (Jusup et al., 2011, 2014). To satisfy the energetic demands of fast growth, larval and early-juvenile tuna gradually shift to a higher quality prey. This is well-known from PBT domestication efforts in Japan, where a diet that leads to healthy early ontogeny starts with rotifers, and then switches to *Artemia nauplii*, live fish larvae, and minced fish meat (Sawada et al., 2005). The improved assimilation, rather than fast growth per se, ultimately allows tunas to attain large body sizes. A more subtle consequence of the said transformations is that the simultaneous improvement of energy assimilation and utilisation rates leaves the reserve capacity unchanged. Tunas are thus large-bodied fish with the reserve capacity similar to their much smaller relatives, making them more prone to starvation. The effect is more pronounced in bluefin than skipjack tuna.

To illustrate the case in point, we provide some examples. According to DEB theory, reserve capacities should obey an interspecies scaling relationship, which states that larger species have a larger reserve capacity (Kooijman, 2010). For example, the online add_my_pet library (Marques et al., 2018) shows that European anchovy (*Engraulis encrasicolus*), a fish with the ultimate length of 18 cm, has the reserve capacity of $[E_M]$=572 J·cm^{-3}. This should be contrasted with the reserve capacity of $3.2 \cdot 10^4$ J·cm^{-3} in bull shark (*Carcharhinus leucas*), which grows to the ultimate length of 320 cm. That the reserve capacity in tunas is an exception to expected scaling is best illustrated by ABT, which has the estimated reserve capacity of 1371 J·cm^{-3} despite the potential to grow up to 372 cm fork length.

Large body size without a correspondingly high reserve capacity makes all three tunas vulnerable to starvation. Experimental evidence in this context shows that a number of SKJ (44.1 cm fork length on average) in a starvation experiment died within the first week of fasting (Boggs & Kitchell, 1991). This is close to our calculated period of 10 days to reserve

depletion. A newer study on post-larval PBT (5.7 cm body length on average) revealed significant stress after 1-2 days of starvation, with almost all fish dying after 8 days without food (Honryo et al., 2018). Here we emphasise that the time to reserve depletion almost surely underestimates the moment at which fish die because starvation blurs the distinction between reserve and structure. The model also does not account for behavioural adaptations, such as reduced activity (Boggs & Kitchell, 1991), aimed at conserving energy. In addition to the small reserve capacity, the vulnerability of the three studied species to starvation is further exacerbated by their high maintenance requirements, which is reflected not only in the estimated times to reserve depletion, but also high supply stress and feed conversion ratios (Fig. S5). Overall, our results theoretically underpin the description of tuna fish as "energy speculators" (e.g., Korsmeyer et al., 1996). Tunas must constantly search for prey out of necessity, which is supported by observations of the continuous feeding success of tagged PBT (Whitlock et al., 2015).

4.2 Ontogenetic shift from ectothermy to heterothermy

Our model indicates that the somatic maintenance cost dramatically increases in early juveniles, shortly after the larval stage. During this period of life, bluefin tunas grow about 10-fold (from about 4 cm to 40 cm fork length) and make an ontogenetic shift from ectothermy to heterothermy (Kubo et al., 2008). Such a shift is consistent with the increased heat dissipation caused by the higher maintenance cost. A reason for this is that heterothermy requires not only good heat conservation (which is a function of countercurrent exchangers known as rete mirabile), but also a significant source of heat for thermogenesis. Such a heat source is the red muscle tissue that tunas possess in excess of other fish species, which also happens to develop in parallel with the said shift from ectothermy to heterothermy (Kubo et al., 2008).

If early juvenile bluefin tuna are to keep growing in the face of the increased maintenance

cost, especially at high growth rates also recorded during this period of life, maintenance needs must be met with higher ingestion and assimilation rates. We estimate using the model that the maximum increase in energy ingestion, obtained by numerically searching for L when $d\dot{p}_A/da=0$, in SKJ, PBT, and ABT happens respectively at 15 cm, 24 cm, and 30 cm fork length. Incidentally, the stomach contents analyses of juvenile PBT show an ontogenetic dietary shift at around 25 cm fork length (Shimose et al., 2013). Smaller PBT (20-25 cm fork length) preyed predominantly upon small squid (juvenile *Enoploteuthis chunii*) or small zooplankton (crustacean larvae) depending on the geographic location, but as they got larger (25-40 cm fork length), they started feeding on mesopelagic (*Maurolicus japonicus*) or epipelagic fish (such as *Etrumeusteres*, *Sardinops melanostictus*, and *Engraulis japonicus*). This ontogenetic dietary shift has also been confirmed by the measurements of nitrogen and carbon isotopes in the white muscle of juvenile PBT (Kitagawa & Fujioka, 2017). Juvenile ABT make a similar shift; the proportion of crustaceans in their stomach contents decreases between 21 cm and 35 cm fork length (Sinopoli et al., 2004). We therefore hypothesize that the increased energy demand during the ontogenetic shift from ectothermy to heterothermy in bluefin tunas is satisfied by a concurrent dietary shift.

The DEB model for SKJ predicts qualitatively the same increase in the somatic maintenance cost as the models for bluefin tunas, but at a somewhat smaller size. This is consistent with the observation of functioning heterothermy in juvenile black skipjack tuna (*Euthynnus lineatus*; a close relative to SKJ) larger than 10 cm fork length (Dickson et al., 2000). The energy demand of the increased somatic maintenance in SKJ may also be supported by a dietary shift, but we found no information to support this.

Interestingly, the increase in the somatic maintenance cost of bluefin tunas happens in parallel with morphological changes in the aspect ratio of the caudal fin at around 30 cm fork length

(Kitagawa & Fujioka, 2017), further suggesting an ontogenetic locomotory shift. The synchronization of various ontogenetic shifts (heterothermy, diet, and locomotion) is suspected to greatly improve the chances of feeding on more nutritious prey, as well as the ability to undertake large scale migrations (Watanabe et al., 2015).

4.3 Evolutionary considerations

Energy allocation to reproduction in all three studied species is such that fecundity is close to the theoretical maximum. This is by no means a general rule. Loggerhead turtles, for example, would maximise fecundity at κ=0.35, but this parameter has been estimated at κ=0.65, reflecting a tradeoff between fecundity and survival (Marn et al., 2017). More specifically, evolution generally acts to maximise fitness—i.e., a combined effect of fecundity and survival—rather than solely fecundity or solely survival (Metz et al., 1992). Loggerhead turtles could perhaps increase their fecundity if κ were smaller, but this would also imply a smaller body size, and thus perhaps higher vulnerability to predation. The κ value of 0.65 in loggerhead turtles, therefore, seems to balance fecundity with survival to produce the maximum fitness.

Why then would evolution in tunas maximise reproductive output? We hypothesise that the answer lies in the large size of these fish. Even if higher fecundity came at the expense of body size, tunas are already large enough that the effect of a smaller size on their survival could be outweighed by the gain in fecundity. If our hypothesis were true, then maximising fitness would be equivalent to maximising fecundity, thus immediately accounting for the results obtained herein. Furthermore, because the large body size of tunas is strongly related to morphological and physiological transformations in the larval stage, we conclude that this short period in the life of an individual tuna critically shapes not just the remainder of a particular tuna's life history, but also the evolution of the whole species.

5. Conclusion

At the heart of the present study is the causation between the characteristics of larval and early juvenile tuna and the characteristics of adult tuna. This causation is threefold:

- Tuna larvae undergo morphological and physiological transformations that increase energy assimilation (input into reserve) and utilisation (output from reserve). The increase is dramatic. By the end of the larval stage, for example, SKJ, PBT, and ABT assimilate energy at rates $M_1\{\dot{p}_{Am}\}$=2273 J·cm^{-2}·d^{-1}, 3137 J·cm^{-2}·d^{-1}, and 3009 J·cm^{-2}·d^{-1}, respectively, while the average for eight species of Mediterranean Perciformes is 429 J·cm^{-2}·d^{-1}, ranging between 258-721 J·cm^{-2}·d^{-1} (Lika). More assimilated energy directly translates into the scope for growth, although how much of that scope is realised depends on energy expenditures too (see Eq. (5)). The reserve capacity, by contrast, remains untouched if inputs into and outputs from reserve increase simultaneously, which is also seen from equation $[E_m]=\{\dot{p}_{Am}\}/\dot{v}$ for the reserve capacity from which factor M_1 that reflects the effects of morphological and physiological changes in the larval stage on energy assimilation and utilisation is absent. Larval ontogeny thus expands the scope for growth, while keeping the reserve capacity constant, implying that adult tunas are large-bodied fish with small reserve.

- The ontogenetic shift from ectothermy to heterothermy in early juveniles requires not only a heat conservation mechanism, but also a powerful source of heat for thermogenesis. The role of the heat source is played by the red muscle tissue, which tunas possess in excess of other fish species (Graham & Dickson, 2004), and which develops in parallel with the ontogenetic shift from ectothermy to heterothermy (Kubo et al., 2008). This is reflected in the steep increase of somatic maintenance costs in energy budgets of all three studied species right after the larval stage (Fig. 2). Early-juvenile ontogeny thus

boosts energy expenditure in tunas, which in conjunction with small energy reserve, accounts for the voracious appetite of these top predators in the later stages of life.

- We have seen that the increase in energy assimilation during the larval stage expands the scope for growth, thus helping tunas to achieve large adult sizes. Meanwhile, it is well known that large-bodied adult fish enjoy higher survival (Pauly, 1980) and fecundity (Barneche). These characteristics, in turn, are the key determinants of population growth and thus of evolutionary fitness as well (Metz et al., 1992). Because natural selection acts to maximise fitness, rather than either survival or fecundity alone, it is rather puzzling why in tunas fecundity would approach the theoretical maximum (Fig. 5). In most species, in fact, allocation fraction κ is far from the value that maximises reproductive output (Kooijman & Lika, 2014). Our results suggest that the explanation for this conundrum lies precisely in the expanded post-larval scope for growth by which adult tunas get big enough that changes in ultimate size minimally affect survival. This frees natural selection to maximise the remaining fitness determinant, that is, fecundity.

Many Actinopterygii, i.e., ray-finned fish, share similar life-history characteristics as tunas. Specifically, neither their small egg size nor small size at first feeding nor small energy reserve show any discernible correlation with the body size of adults (Kooijman & Lika, 2014). The listed characteristics therefore pertain, with isolated exceptions, to the whole class of ray-finned fish. What truly sets tunas apart from their phylogenetic relatives is the post-larval ability to assimilate energy which, as we have seen above, is almost an order of magnitude larger in the three studied tuna species than the eight species of Mediterranean Perciformes for which the data is readily available (Lika). The improved ability to assimilate energy allows adult tunas to grow large, which then conspires with the small reserve capacity and the high energy expenditure to dictate the ecology (e.g., voracious appetite and

vulnerability to starvation) as well as the evolution (e.g., high fecundity) of these fish.

Acknowledgments

We thank H. Ijima, H. Matsuda, and T. Klanjšček for useful discussions. M.J. was supported by the Research Grant Program of Inamori Foundation. T.K. was partially supported by CREST funding program from Japan Science and Technology Agency (JST), grant-in-aid for Scientific Research (A) (No. 16H01769), and grant-in-aid for Scientific Research (B) (No. 24380104) from the Japan Society for the Promotion of Science (JSPS).

Author's contributions

Y.A., M.J., and A-E.N. conceived the research; Y.A. and M.J. conducted simulations; all authors interpreted the results and wrote the manuscript. Y.A. and M.J. contributed equally.

Data Accessibility

All data is available upon request from the corresponding author.

References

Aoki, Y., Kitagawa, T., Kiyofuji, H., Okamoto, S., & Kawamura, T. (2017). Changes in energy intake and cost of transport by skipjack tuna (*Katsuwonus pelamis*) during northward migration in the northwestern Pacific Ocean. *Deep Sea Research Part. II: Topical Studies in Oceanography*, 140, 83-93. doi:10.1016/j.dsr2.2016.05.012

Augustine, S. (2017). Maturity as quantifier for physiological time: Comment on "Physics of metabolic organization" by Marko Jusup et al. *Physics of Life Reviews*, 20, 40-42.

Barneche, D.R., Robertson, D.R., White, C.R., & Marshall, D.J. (2018) Fish reproductive-energy output increases disproportionately with body size. *Science*, 360(6389), 642-645.

Boggs, C. H. & Kitchell, J. F. (1991). Tuna metabolic rates estimated from energy-losses during starvation. *Physiological Zoology,* 64, 502-524.

Carey, F. G., & Teal, J. M. (1966). Heat conservation in tuna fish muscle. *Proceedings of the National Academy of Sciences of the United States of America*, 56, 1464-1469.

Dewar, H., & Graham, J. B. (1994). Studies of tropical tuna swimming performance in a large water tunnel. I. Energetics. *Journal of Experimental Biology*, 192, 13-31.

Dickson, K. A., Johnson, N. M., Donley, J. M., Hoskinson, J. A., Hansen M. W, & Tessier, J. (2000). Ontogenetic changes in characteristics required for endothermy in juvenile black skipjack tuna (*Euthynnus lineatus*). *Journal of Experimental Biology*, 203, 3077-3087.

Garland, T. Jr., & Carter, P. A. (1994). Evolutionary physiology. *Annual Review of Physiology* 5, 579-621. doi:10.1146/annurev.ph.56.030194.003051

Graham, J. B., & Dickson, K. A. (2004). Tuna comparative physiology. *Journal of Experimental Biology*, 207 (23), 4015-4024. doi:10.1242/jeb.01267

Honryo, T., Oakada, T., Kawahara, M., Kurata, M., Agawa, Y., Sawada, Y., ... Ishibashi, Y., (2018). Estimated time for recovery from transportation stress and starvation in juvenile Pacific bluefin tuna *Thunnus orientalis*. *Aquaculture*, 484, 175-183.

Hunter, J. R., Macewicz, B. J. & Sibert, J. R. (1986). The Spawning Frequency of Skipjack Tuna, *Katsuwonus pelamis*, from the South Pacific. *Fishery Bulletin*, 84, 895-903.

Jusup, M., Klanjšček, T., Matsuda, H., & Kooijman, S. A. L. M. (2011). A full lifecycle bioenergetic model for bluefin tuna. *Plos One*, 6(7): e21903.

Jusup, M., Klanjšček, T., & Matsuda, H. (2014). Simple measurements reveal the feeding history, the onset of reproduction, and energy conversion efficiencies in captive bluefin tuna. *Journal of Sea Research*, 94, 144-155. doi:10.1016/j.seares.2014.09.002

Jusup, M., & Matsuda, H. (2015). Mathematical modeling of bluefin tuna growth, maturation, and reproduction based on physiological energetics. In Kitagawa, T. & Kimura, S. (Eds.) *Biology and Ecology of Bluefin Tuna* (pp. 369-399). CRC Press, Boca Raton.

Jusup, M., Sousa, T., Domingos, T., Labinac, V., Marn, N., Wang, Z., & Klanjšček, T. (2017). Physics of metabolic organization. *Physics of Life Reviews*, 20, 1-39. doi: 10.1016/j.plrev. 2016.09.001

Kaji, T., 2003. Bluefin tuna larval rearing and development-state of the art. *Cahier Options Méditerranéennes*, 60, pp.85-89.

Kitagawa, T., Kato, Y., Miller, M. J., Sasai, Y., Sasaki, H., & Kimura, S. (2010). The restricted spawning area and season of Pacific bluefin tuna facilitate use of nursery areas: A modeling approach to larval and juvenile dispersal processes. *Journal of Experimental Marine Biology and Ecology*, *393*(1), 23-31.

Kitagawa, T., & Fujioka, K. (2017). Rapid ontogenetic shift in juvenile Pacific bluefin tuna

diet. *Marine Ecology Progress Series*, 571, 253-257. doi:10.3354/meps12129

Kooijman, S. A. L. M. (2009). What the egg can tell about its hen: embryonic development on the basis of dynamic energy budgets. *Journal of Mathematical Biology*, 58(3), 377-394.

Kooijman, S. A. L. M. (2010). *Dynamic energy budget theory for metabolic organisation* (3rd ed). Cambridge University Press.

Kooijman, S. A. L. M., & Lika, K. (2014). Comparative energetics of the 5 fish classes on the basis of dynamic energy budgets. *Journal of Sea Research*, *94*, 19-28. doi: 10.1016/j.seares.2014.01.015.

Korsmeyer, K. E., Dewar, H., Lai, N. C., & Graham, J. B. (1996). The aerobic capacity of tunas: adaptation for multiple metabolic demands. *Comparative Biochemistry and Physiology A*, 113(1), 17-24. doi: 10.1016/0300-9629(95)02061-6

Kubo, T., Sakamoto, W., Murata, O., & Kumai, H. (2008). Whole□body heat transfer coefficient and body temperature change of juvenile Pacific bluefin tuna *Thunnus orientalis* according to growth. *Fisheries Science*, *74*(5), 995-1004.

Lika, K., Kearney, M. R., Freitas, V., van der Veer, H. W., van der Meer, J., Wijsman, J. W., ... Kooijman, S. A. L. M. (2011). The "covariation method" for estimating the parameters of the standard Dynamic Energy Budget model I: philosophy and approach. *Journal of Sea Research*, 66(4), 270-277. doi: 10.1016/j.seares.2011.07.010

Lika, K., Kooijman, S.A. and Papandroulakis, N. (2014a) Metabolic acceleration in Mediterranean perciformes. *Journal of Sea Research*, 94, 37-46.

Marn, N., Kooijman, S. A. L. M., Jusup, M., Legović, T., & Klanjšček, T. (2017). Inferring physiological energetics of loggerhead turtle (*Caretta caretta*) from existing data using a general metabolic theory. *Marine Environmental Research*, 126, 14-25. doi: 10.1016/

j.marenvres.2017.01.003

Marques, G. M. (2017). Constraints and DEB parameter estimation. Comment on “Physics of metabolic organization” by Marko Jusup et al. *Physics of life reviews*, 20, 66-68.

Marques, G.M., Augustine, S., Lika, K., Pecquerie, L., Domingos, T. and Kooijman, S.A., 2018. The AmP project: Comparing species on the basis of dynamic energy budget parameters. *PLoS computational biology*, *14*(5), p.e1006100.

Masuma, S. (2009). Biology of Pacific bluefin tuna inferred from approaches in captivity. *Collect Vol Sci Pap ICCAT*, 63, 207-229.

Matsumoto, W., M, Skillman, R.A., & Dizon, A., E (1984). Synopsis of biological data on skipjack tuna, *Katsuwonus pelamis*. *U.S. Dept. of Commerce, National Oceanic and Atmospheric Administration Technical Report National Marine Fisheries Services Circular*, 451, 92.

Metz, J. A., Nisbet, R. M., & Geritz, S. A. (1992). How should we define ‘fitness’ for general ecological scenarios? *Trends in Ecology & Evolution*, 7(6), 198-202.

Miyashita, S., Sawada, Y., Okada, T., Murata, O., & Kumai, H. (2001). Morphological development and growth of laboratory-reared larval and juvenile *Thunnus thynnus* (Pisces: *Scombridae*). *Fishery Bulletin*, *99*(4), 601-617.

Nisbet, R. M., Muller, E. B., Lika, K., & Kooijman, S. A. L. M. (2000). From molecules to ecosystems through dynamic energy budget models. *Journal of Animal Ecology*, 69(6), 913-926. doi: 10.1111/j.1365-2656.2000.00448.x

Pauly, D. (1980). On the interrelationships between natural mortality, growth parameters, and mean environmental temperature in 175 fish stocks. *ICES Journal of Marine Science*, 39(2), 175-192.

Santamaria, N., Bello, G., Corriero, A., Deflorio, M., Vassallo-Agius, R., Bok, T., & De Metrio, G. (2009). Age and growth of Atlantic bluefin tuna, *Thunnus thynnus* (*Osteichthyes*: *Thunnidae*), in the Mediterranean Sea. *Journal of Applied Ichthyology*, 25, 38-45. doi: 10.1111/j.1439-0426.2009.01191.x

Sawada, Y., Okada, T., Miyashita, S., Murata, O., & Kumai, H. (2005). Completion of the Pacific bluefin tuna *Thunnus orientalis* (Temminck et Schlegel) life cycle. *Aquaculture Research*, 36, 413-421.

Schmidt-Nielsen, K. (1972). Locomotion: Energy cost of swimming, flying, and running. *Science*, 177, 222-228. doi: 10.1126/science.177.4045.222

Shimose, T., Watanabe, H., Tanabe, T., & Kubodera, T. (2013). Ontogenetic diet shift of age-0 year Pacific bluefin tuna *Thunnus orientalis*. *Journal of Fish Biology*, 82, 263-276. doi: 10.1111/j.1095-8649.2012.03483.x

Sinopoli, M., Pipitone, C., Campagnuolo, S., Campo, D., Castriota, L., Mostarda, E., & Andaloro, F. (2004). Diet of young-of-the year bluefin tuna, *Thunnus thynnus* (Linnaeus, 1758), in the southern Tyrrhenian (Mediterranean) Sea. *Journal of Applied Ichthyology*, 20, 310-313.

Watanabe, Y. Y., Goldman, K. J., Caselle, J. E., Chapman, D. D., & Papastamatiou, Y. P. (2015). Comparative analyses of animal-tracking data reveal ecological significance of endothermy in fishes. *Proceedings of the National Academy of Sciences of the United States of America*, 112:6104-6109.

Whitlock, R. E., Hazen, E. L., Walli, A., Farwell, C., Bograd, S. J., Foley, D. G., ... Block, B. A. (2015). Direct quantification of energy intake in an apex marine predator suggests physiology is a key driver of migrations. *Science Advances*, 1. doi: 10.1126/sciadv.1400270

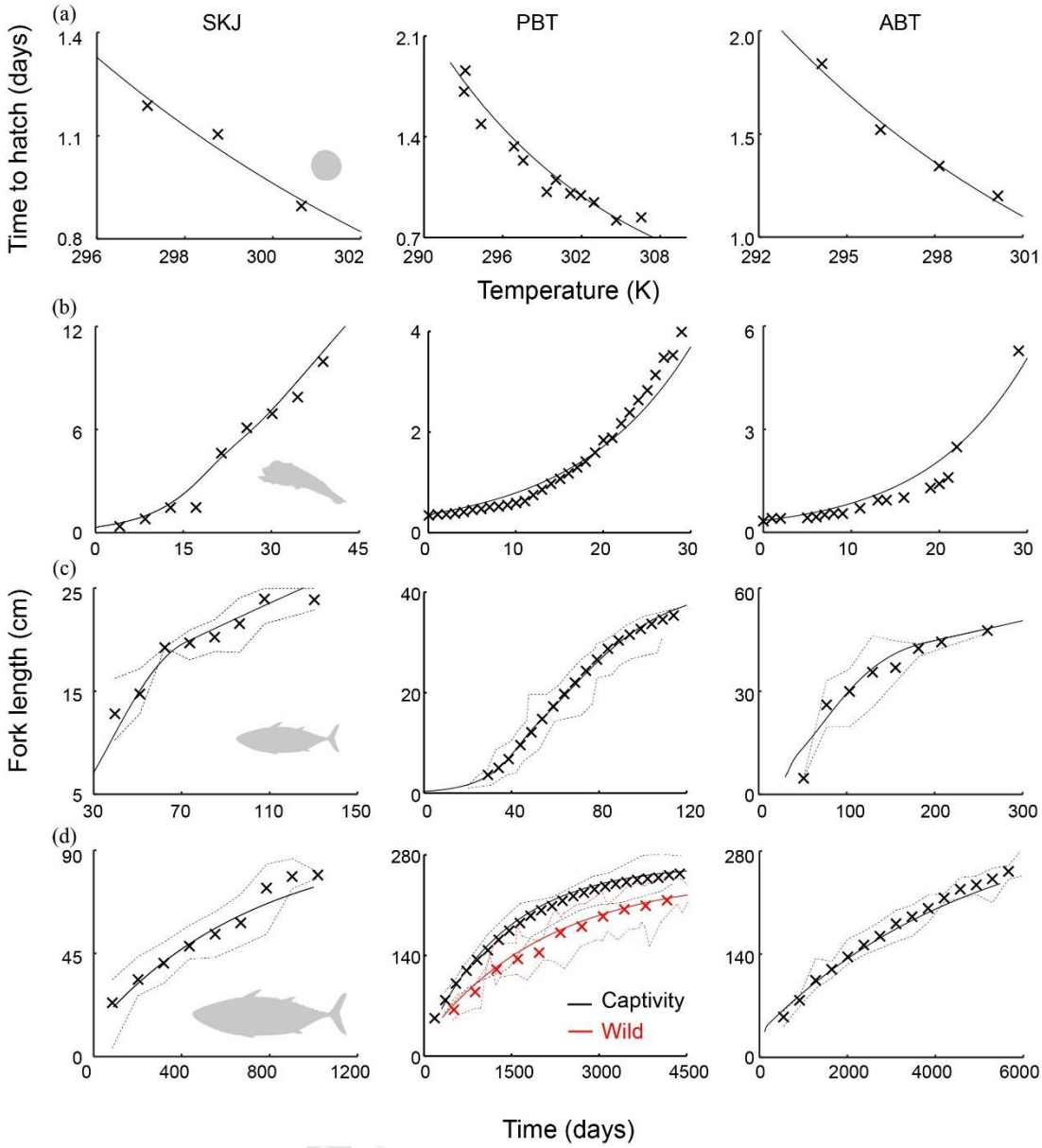

Figure 1. Goodness of fit I. Model estimates for skipjack (left; SKJ), Pacific bluefin (middle; PBT), and Atlantic bluefin (right; ABT) tunas compared to observational data: (a) time to hatch as a function of water temperature; growth in (b) larval, (c) juvenile and (d) adult stages as the functions of time since hatching. Model estimates, averaged data, and data scatter (observed minima and maxima) are respectively represented as solid curves, x-marks, and dashed envelopes. For PBT, black and red colours indicate data on wild and captive fish, respectively, where only the latter was used in model fitting.

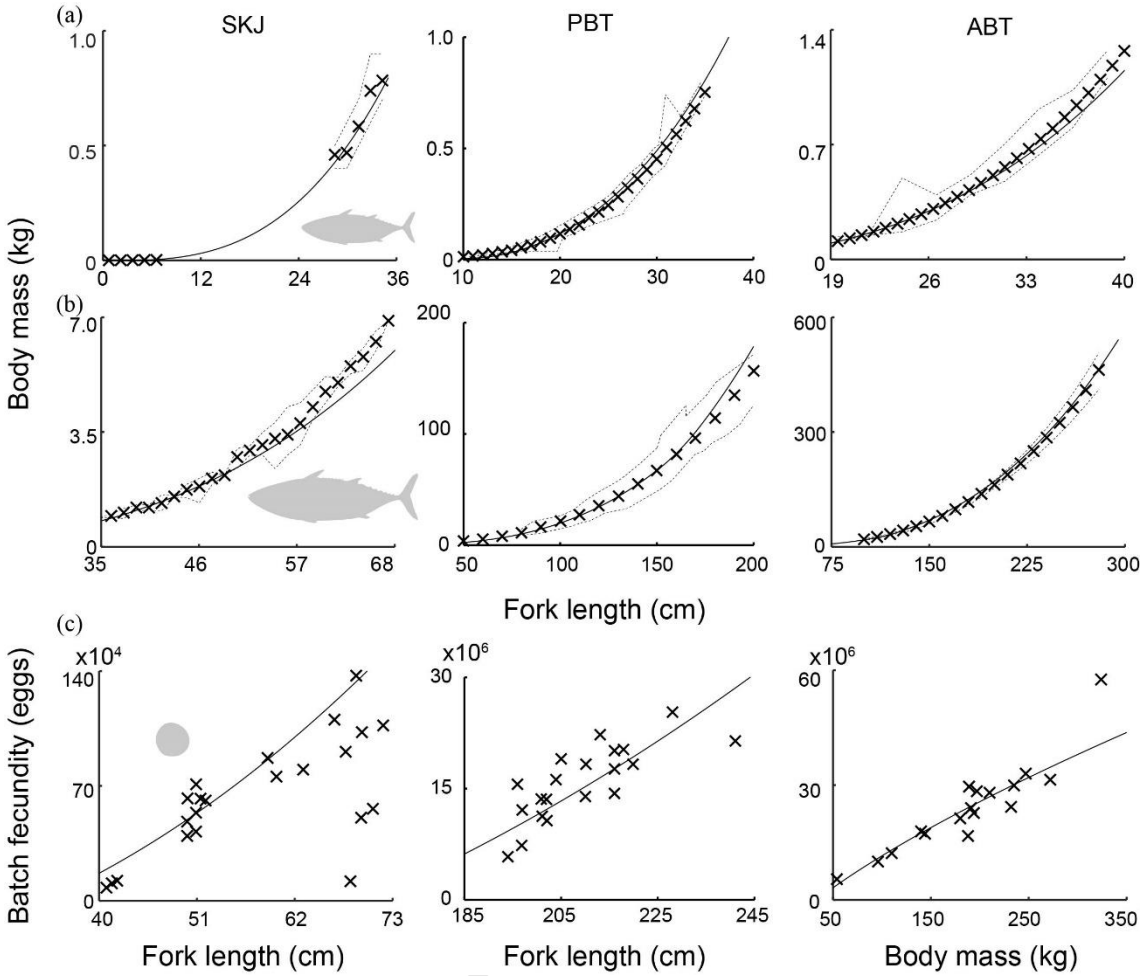

Figure 2. Goodness of fit II. Model estimates for skipjack (left; SKJ), Pacific bluefin (middle; PBT), and Atlantic bluefin (right; ABT) tunas compared to observational data: body mass as a function of fork length, often referred to as the weight-length relationship, in (a) juvenile and (b) adult stages; (c) batch fecundity as a function of body size. In (c), body mass is used as a size indicator for ABT instead of fork length due to data availability. Model estimates, averaged data, and data scatter (observed minima and maxima) are respectively represented as solid curves, x marks, and dashed envelopes, except for batch fecundity plots where raw data (x marks) were used.

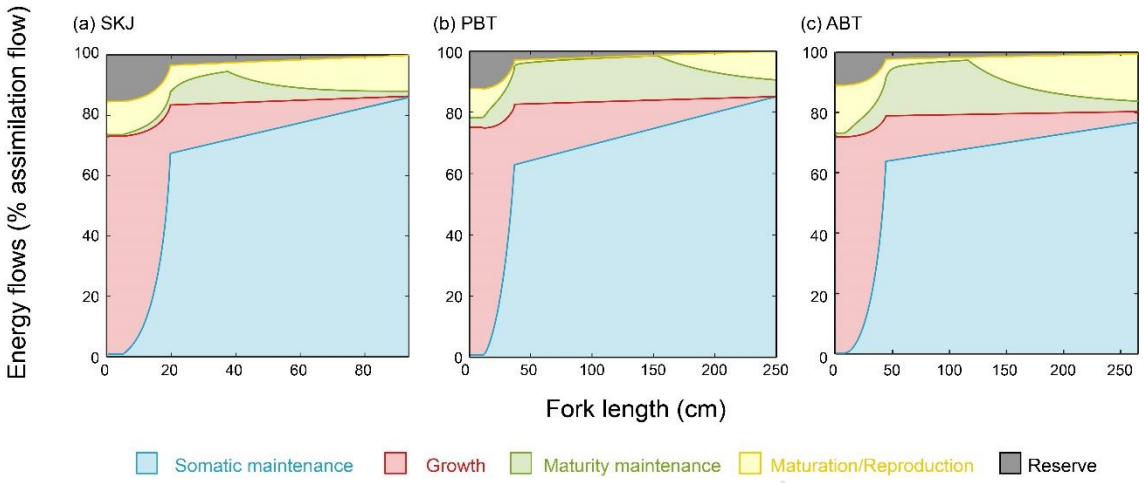

Figure 3. Energy budgets of three commercial tuna species. Plots indicate energy investments into various metabolic processes relative to energy assimilation: (a) skipjack (SKJ), (b) Pacific bluefin (PBT), and (c) Atlantic bluefin (ABT) tunas. The dark gray area on top represents the difference between assimilation and utilization flows used to build up reserve. The utilization flow is divided between the maturation/reproduction flow (yellow), the maturity maintenance flow (green), the growth flow (red), and the somatic maintenance flow (blue). We assumed food availability that fish experience in the wild, which we estimate at f=0.925 for skipjack, f=0.905 for Pacific bluefin, and f=0.950 for Atlantic bluefin tuna.

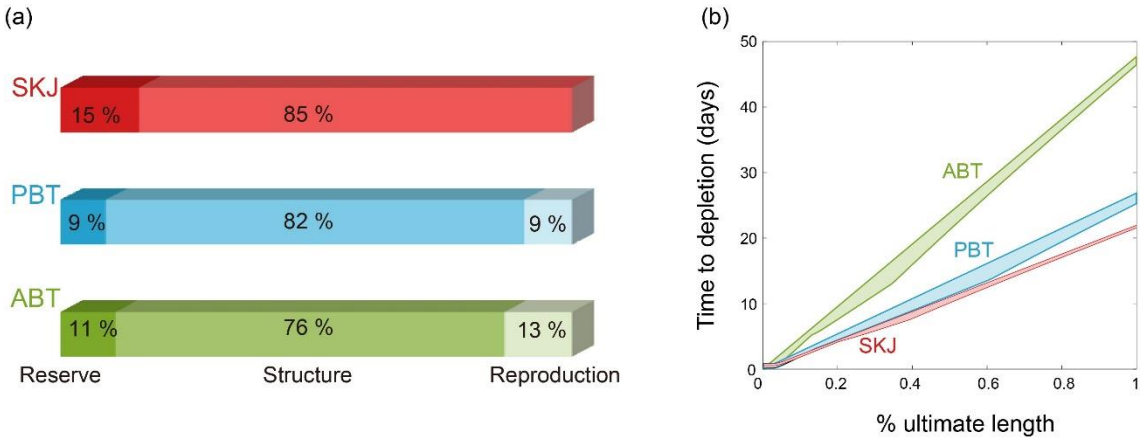

Figure 4. Reserve size and the ability to handle starvation. Plots show (a) the percentage of body mass attributable to reserve (left), structure (middle), and the reproductive buffer (right) at maximum size; (b) the time to reserve depletion as a function of fork length for skipjack (red; SKJ), Pacific bluefin (blue; PBT), and Atlantic bluefin (green; ABT) tunas. The relative contribution of reserve and structure to body mass is independent of size at constant food availability. By contrast, the contribution of reproductive buffer increases with size. We assume that starvation begins when the utilization flow is insufficient to satisfy somatic maintenance (i.e., when reserve energy is $E^*=\dot{p}_S L/\kappa\dot{v}$) and that starving fish draw energy from reserve to satisfy either (i) somatic maintenance only or (ii) somatic and maturity maintenance. Lower and upper boundaries of the estimated times to reserve depletion correspond to (i) and (ii), respectively.

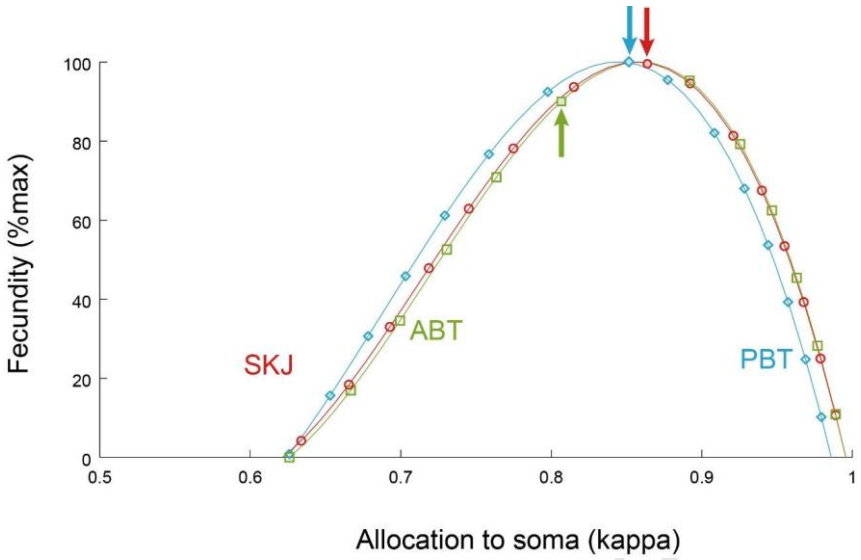

Figure 5. Reproductive potential and the actual reproductive output of three commercial tuna species. Fecundity relative to the theoretical maximum as a function of allocation to soma (κ) for skipjack (red circles; SKJ), Pacific bluefin (blue diamonds; PBT), and Atlantic bluefin (green squares; ABT) tunas. Arrows indicate the actual reproductive output of each species based on the estimated value of κ. Displayed curves are concave because at high κ values, fish grow large by investing into growth instead of reproduction, whereas at low κ values, inadequate growth limits energy assimilation and thus the reproductive output as well. Estimated κ for bluefin tunas is very close to the optimal value.

Table 1. Goodness of fit III. Comparison of model-estimated and observed life history traits for the three studied bluefin tuna species: skipjack (SKJ), Pacific bluefin (PBT), and Atlantic bluefin (ABT) tuna.

	SKJ		PBT		ABT	
Data	Model	Literature	Model	Literature	Model	Literature
Egg dry mass	42.8	42.8[a]	64.49	N/A[*]	60.49	61.8[i], 63.4[i]
Length at hatching	0.2669	0.265[a]	0.2975	0.308[e]	0.3324	N/A[**]
Length at birth	0.3670	0.37[a]	0.3985	0.391[e]	0.3572	N/A[**]
Length at puberty	37.5	37.5[b]	152.2	159[f]	116.2	115[j], 135[k]
Ultimate length	95.34	93.6[c]	261	265[g]	334.5	372[l]
Ultimate body mass	15.31	10.4[d]	413.5	450[h]	617.5	685[j]

[a]Egg dry mass for skipjack was borrowed from the same tropical species of yellowfin tuna (*T.albacares*, Margulies et al., 2007) due to data availability; [b]Kayama (2006), [c]Tanabe, Kayama, & Ogura (2003), [d]Uchiyama & Kazama (2003), [e]Sawada et al. (2005), [f]Tanaka (1999), [g]Masuma (2009), [h]Bayliff (2001), [i]Anon (2010), [j]Fromentin and Fonteneau (2001), [k]Corriero et al.(2005), [l]Santamaria et al. (2009).

[*]Information taken from the data on ABT due to limited data availability.

[**]Information taken from the data on PBT due to limited data availability.

Highlights

- We inferred energy budgets of skipjack, Pacific bluefin, and Atlantic bluefin tuna.
- Morphological and physiological adaptations accelerate ontogeny in the larval stage.
- Accelerated ontogeny expands tuna scope for growth, but leaves energy reserve small.
- Thermogenesis that starts in early juveniles is a considerable energy sink.
- Large body, small reserve, and high energy costs shape tuna ecology and evolution.